Deformation measurement using SAR interferometry: quantitative aspects

Michele Crosetto[(1)], Erlinda Biescas[(1)], Ismael Fernández[(1)], Ivan Torrobella[(1)], Bruno Crippa[(2)]

[(1)] *Institute of Geomatics, Avinguda del Canal Olímpic s/n, E-08860 Castelldefels (Barcelona), Spain*
Email: michele.crosetto@ideg.es, erlinda.biescas@ideg.es
[(2)] *Department of Earth Sciences, University of Milan, Via Cicognara 7, I-20129 Milan, Italy*
Email: bruno.crippa@unimi.it

ABSTRACT

This paper addresses some key aspects of the quantitative measurement of land deformations using differential SAR interferometry. In the introduction, the most important quality aspects of deformation monitoring, i.e. the precision, accuracy and reliability of the estimates, are concisely described. Then a description of the main DInSAR techniques proposed in literature is given, addressing the fundamental aspect of the selection of the most suitable observations for the deformation estimation. This is followed by a discussion on the DInSAR capability to support a quantitative monitoring of deformations. In the last part is illustrated an example of DInSAR subsidence estimation based on multiple ascending and descending ERS SAR images, where the results obtained independently with the ascending and descending data are compared. Furthermore, the analysis of the atmospheric component performed over a stable area, is illustrated.

1. INTRODUCTION: PRECISION, ACCURACY AND RELIABILITY

This paper addresses some aspects of the quantitative measurement of terrain deformations using the differential interferometric SAR (DInSAR) technique. This technique has demonstrated its capability to measure deformations in a wide range of applications, which include urban subsidences related to water resource exploitation [1], mining activity [2], and construction works [3]; landslides; earthquakes [4]; volcanoes [5]; glacier dynamics [6]; etc. These applications, which extend to many forms of surface deformation and to various geophysical phenomena, require different quality levels to the estimates provided by DInSAR. For the purposes of some applications a qualitative use of the DInSAR results seems to be sufficient. However, this is certainly not the case for some other important applications, like those related to risk assessment and public safety, which need to be characterised by high quality standards. In fact, a valuable support to the decision makers in risk management may be only provided by a fully quantitative estimate of the deformation phenomena, which involves a thorough characterisation of the estimation quality. High quality standards in deformation monitoring are usually achieved by different types of geodetic techniques. In geodesy, three important quality aspects are typically considered: the precision, accuracy and reliability of the estimates. It is evident that for the DInSAR technique, which is claimed to provide "geodetic quality", the same quality aspects should be considered. This is usually not the case, since in the literature there is even some confusion associated with the use of the above mentioned terms.

Considering a simple case, where DInSAR observations are used to estimate the maximum deformation of a given subsidence, we briefly remind the definitions of the three above terms, as they usually are employed in geodesy and in other scientific fields. The term precision refers to the dispersion of the estimate of a given parameter. A measure of the dispersion is the variance. The accuracy is the extent to which the mean of the population of the estimate approaches the true value of the parameter. Finally, the reliability refers to the robustness of a given technique against not modelled errors in the observations. Back to the considered case, the precision of the measure of the deformation can be evaluated from the precision of the DInSAR observations (e.g. from the variance of the DInSAR phase), typically using the law of the variance propagation [7], or other numerical methods for error propagation [8]. Note that the precision represents the result of an estimation procedure, which is strictly dependent on the model which connects the DInSAR observations and the estimated parameter, and on the stochastic model which describes the uncertainty of the DInSAR observations. Examples of biased (non accurate) precisions typically result from disregarding the correlations between the errors associated with the DInSAR observations.

The accuracy of the estimate, on the contrary, cannot be assessed by simple error propagation and requires a validation based on independent data of higher quality. It is therefore evident that precision and accuracy are not synonymous (there

Proc. of FRINGE 2003 Workshop, Frascati, Italy,
1 – 5 December 2003 (ESA SP-550, June 2004) 65_crose

are examples of instruments which are highly precise, but not at all accurate). It is important to underline that in the DInSAR applications a fully quantitative validation is very rarely performed. Notwithstanding this fact, it is not rare to find papers and presentations where millimetric (per year), or even sub-millimetric (per year) DInSAR accuracy is claimed: they most probably refer to the precision of the (deformation velocity) estimates, and not to their accuracy. Finally, concerning the reliability, it depends on the redundancy of the observations. The results of many DInSAR applications are derived using a single interferometric pair that represents a typical zero redundancy configuration, with which it is not possible to check the presence of important sources of errors, like the atmospheric artefacts. In these cases we can say that the deformation estimates are not reliable. Note that the same occurs for the digital elevation models (DEMs) derived with single InSAR pairs, where atmospheric artefacts can be interpreted, e.g. as topographical depressions.

This paper begins with a brief description of the main DInSAR procedures described in literature. This section addresses the important aspect of the selection of the observations that are suitable for estimating the deformation. This is followed by a discussion on the DInSAR capability to support a quantitative monitoring of deformations. In the last part of the paper is illustrated an example of DInSAR subsidence estimation based on stacks of ascending and descending ERS SAR images.

2. DInSAR TECHNIQUES

Since the first description of the DInSAR technique [9], different types of methods have been developed and the capabilities of DInSAR have improved considerably. The DInSAR techniques can be divided in three classes: the classical DInSAR configuration, i.e. the coherence-based DInSAR with a single image pair; the coherence-based techniques with multiple images; and the DInSAR techniques based on the so-called Permanent Scatterers (PS) extracted on multiple images. There are two main aspects that differentiate the above techniques: the criterion adopted in the selection of the suitable pixels and number of required SAR images. The first two types of techniques use the coherence for the pixel selection, while the last class of techniques uses the stability of the SAR amplitude, see [10]. The second aspect is the number of required SAR images. The first class of techniques only requires a couple of images, while the other two classes of techniques use time series of co-registered SAR images, i.e. require much more data (data redundancy). As it is discussed in the following section, this aspect represents the key factor to achieve a quantitative deformation monitoring.

Both the coherent-based and the PS-based techniques with large SAR image stacks provide good results over coherent areas, e.g. urban areas. However, a fundamental factor to extend the DInSAR applicability is the capability to measure deformations in different types of operational context. In particular, the key factor to achieve a high DInSAR flexibility is the capability to observe deformations over low-coherent areas. The PS-based techniques only exploit the targets that show stable SAR amplitude over a time series of images. This criterion is quite selective. On one hand it allows good quality standards to be achieved, while on the other hand it reduces the flexibility of the technique. In fact, outside the urban areas it is quite common to have a low density of PS, which may often be inadequate to sample small-scale deformation phenomena (e.g. subsidences of small spatial extent, small landslides, etc.). This can also occur for the monitoring of specific (user-defined) structures in urban areas. This is illustrated in Fig. 1, considering the city of Barcelona (Spain). In the right side of Fig. 1 is illustrated the coherence of an interferogram with a time interval of 1085 days: there are 142651 pixels (20 by 20 m) of good quality (coherence above 0.6). On the left side are illustrated the PS estimated with 20 images: there are only 5956 of them over the city. It must be noted that this number results from the criterion of [10], selecting the pixels which have an amplitude dispersion index less than 0.25. It seems that this reduced number of pixels can be increased using a more advanced pixel selection (some results were shown during the Fringe 2003 workshop). However, the authors consider that the considerably larger number of “good pixels” of the coherence-based vs. PS-based techniques can make the difference in the capability of DInSAR to support certain types of applications. An additional advantage of the coherence-based techniques is that they may also work with limited sets of SAR images.

3. QUANTITATIVE DEFORMATION MONITORING

The key factor to achieve a quantitative DInSAR deformation monitoring is the number of available interferograms (i.e. observations). The classical DInSAR configuration is based on a single interferogram. This is the simplest DInSAR configuration, which often is the only one that can be implemented, due to the limited data availability for several practical deformation measurement applications. As already mentioned in the introduction, with this configuration it is not possible to check the presence of the different errors that may affect the interferometric observations.

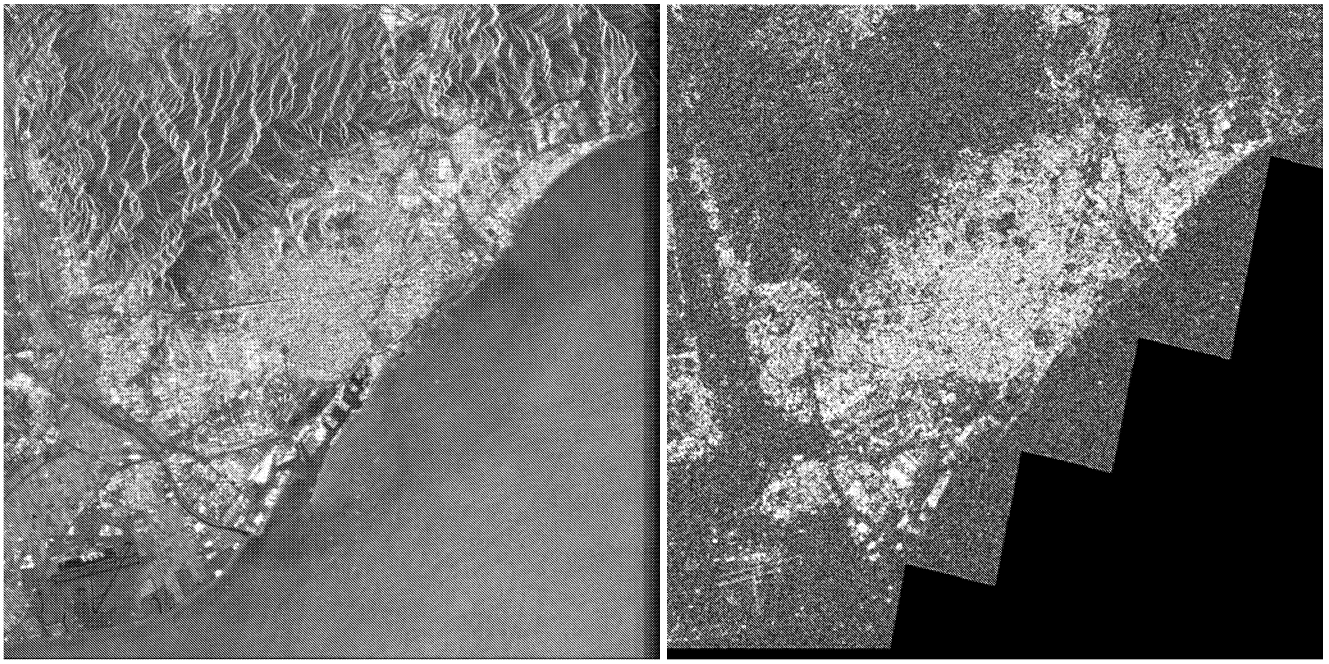

Fig. 1. Comparison of data availability over the Barcelona area. Right: coherence of an ERS-2 interferogram with ΔT=1085 days. The image has 142651 pixels with coherence above 0.6. Left: distribution of the PS estimated with 20 images. There are only 5956 PS with an amplitude dispersion index D_A less than 0.25.

The DInSAR phase (i.e. the main observable of the DInSAR techniques) include error components which have different origins. Among the most important we can include the unwrapping-related errors, the residual topographic component due to DEM errors, and the atmospheric artefacts. The unwrapping-related errors usually occur in low coherence areas, where the interferometric phase noise is high. In order to avoid these areas, the phase unwrapping for sparse data can be used. The residual topographic component can represent an important error source if large baselines are used and the quality of the DEM is not known. Finally, the atmospheric artefacts represent a very important error source, which can strongly degrade the quality of the DInSAR observations. All these error sources represent a strong limitation of the DInSAR technique based on a single interferogram. It is however important to underline that the usefulness of this simple configuration is context dependent. For instance, in all applications with strong deformations (e.g. co-seismic displacements of the order of meters) the magnitude of the above mentioned errors usually does not hide the deformation signal. Furthermore, the availability of a priori information on the phenomenon under analysis may reduce the impact of these errors. For instance, dealing with small-scale subsidences, where the location of stable areas around the subsidence is known, it is possible to reduce the influence of the atmospheric artefacts, see the least squares (LS) collocation procedure described in [2]. The analysis of the DInSAR atmospheric component based on stable areas is illustrated in the following section.

A fully quantitative DInSAR monitoring may only be achieved by using multiple interferograms, i.e. multiple observations of the phenomenon under analysis. However, this is just a necessary condition, which is not sufficient to yield high quality DInSAR results. Two other conditions have to be fulfilled. Firstly, a careful DInSAR processing has to be implemented. The quality of all major processing steps (e.g. image registration, phase unwrapping, etc.) must be controlled through automatic or semi-automatic procedures. Note that the control of the phase unwrapping results may be time consuming. Secondly, suitable data modelling and analysis procedures have to be employed with an appropriate statistical treatment of the DInSAR observations. A detailed description of a data modelling and analysis procedure for DInSAR data is beyond the scope of this paper. We only recall some basic properties that can be exploited. The component of the DInSAR phase related with the (unknown) deformation is usually correlated, spatially and temporally, while the atmospheric component is correlated spatially, and uncorrelated temporally. Furthermore, the residual topographic component is a function of the

normal baseline of each interferogram. In order to exploit these properties the authors have implemented a model, which allows the deformation velocity of each pixel to be modelled by a stepwise linear function, which is estimated by LS adjustment. The LS procedure supports the classical Baarda data snooping [11], useful to detect the unwrapping-related errors. The preliminary results obtained with this method are discussed in the following section.

4. DISCUSSION OF THE RESULTS

This section summarizes some results obtained over a subsidence of small spatial extend (Sallent, Spain), observed by ascending and descending ERS SAR data. First, we briefly discuss the analysis of the atmospheric component of the descending interferograms, which was performed on a stable area located near the village of Sallent. On a stable areas it is possible to estimate the atmospheric component by analysing the spatial autocorrelation of the DInSAR phase [2]. We use for this purpose the autocovariance function. An interferogram weakly affected by atmospheric effects is characterised by a negligible correlation length L_C (see int15, 20 and 95 in Fig.2), while in presence of atmospheric heterogeneities L_C is significantly different from zero (see int4 and 77 in Fig.2). This criterion can be used to classify reliable and potentially degraded interferograms. This information can also be taken into account during the estimation of the subsidence (only if the stable area is located in the vicinity of the subsidence area).

The estimation of the Sallent subsidence was obtained with two independent datasets: 17 ascending interferograms and 9 descending interferograms covering the same period, from 1995 and 2000. The geocoded mean velocity field estimated with the ascending data is shown in Fig. 3. The same figure includes a comparison of the ascending and descending results, showing two profiles over the two geocoded velocity fields. In general, there is a quite good agreement between the two datasets. This is a preliminary comparison, because the descending dataset has a reduced number of interferograms (9 vs. 17). A further step of this research will be the joint estimation of the subsidence velocity field by fusion of the ascending and descending datasets, and the validation of the results using external data, coming from geodetic levelling surveys.

5. ACKNOLEDGMENTS

The descendent ERS SAR data used in this work were provided by ESA in the frame of the project number 16702/02/I-LG “Development of algorithms for the exploitation of the ERS-Envisat data using the stable points network”.

6. REFERENCES

1. Amelung F. et al., Sensing the ups and downs of Las Vegas: InSAR reveals structural control of land subsidence and aquifer-system deformation, Geology, 27(6), 483-486, 1999.
2. Crosetto M. et al., Subsidence monitoring using SAR interferometry: reduction of the atmospheric effects using stochastic filtering, Geophysical Research Letters, 29(9), 26-29, 2002.
3. Tesauro M. et al., Urban subsidence inside the city of Napoli (Italy) observed by satellite radar interferometry, Geophysical. Research Letters, 27(13), 1961-1964, 2000.
4. Massonnet D. et al., Radar interferometry mapping of deformation in the year after the Landers earthquake, Nature, 369, 227-230, 1994.
5. Massonnet D. et al., Deflation of Mount Etna monitored by spaceborne radar interferometry, Nature, 375, 567-570, 1995.
6. Goldstein R.M. et al., Satellite radar interferometry for monitoring ice sheet motion: application to an Antarctic ice stream, Science, 262, 1525-1530, 1993.
7. Hanssen R., Radar interferometry, Kluwer Academic Publishers, Dordrecht, The Netherlands, 2001.
8. Crosetto M. et al., Uncertainty propagation in models driven by remotely sensed data, Remote Sensing of Environment, 76(3), 373-385, 2001.
9. Gabriel A.K. et al., Mapping small elevation changes over large areas: differential radar interferometry, J. of Geophys. Research, 94(B7), 9183-9191, 1989.
10. Ferretti A. et al., Nonlinear subsidence rate estimation using the Permanent Scatterers in differential SAR interferometry, IEEE Transactions on Geoscience and Remote Sensing, 38(5), 2202-2012, 2000.
11. Baarda W., A testing procedure for use in geodetic networks. Netherlands Geodetic Commission – Publications on Geodesy, 2 (5), Delft (Holland), 1968.

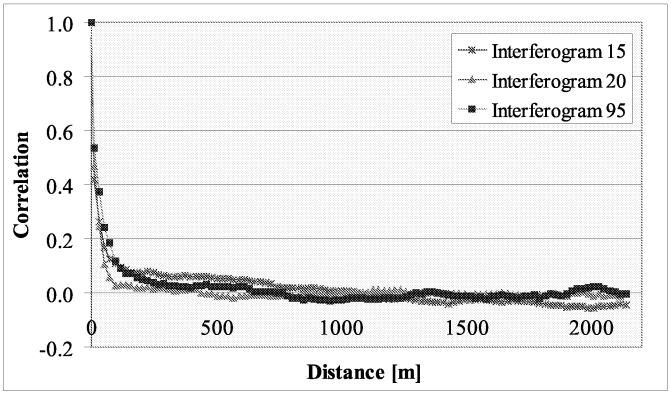

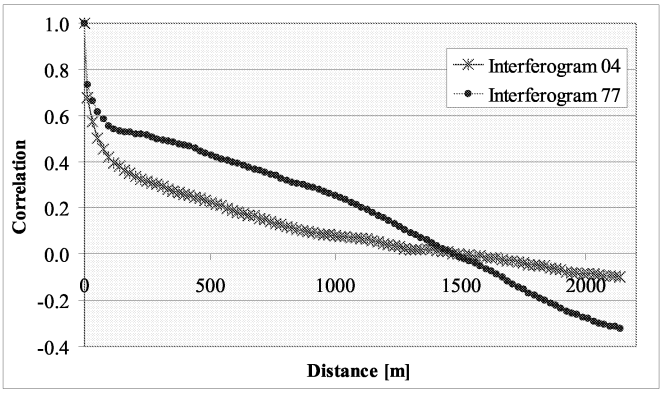

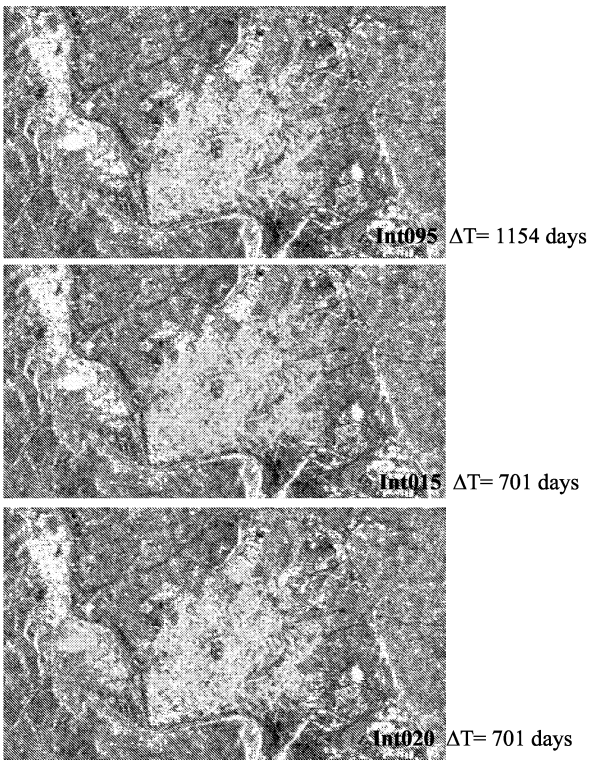

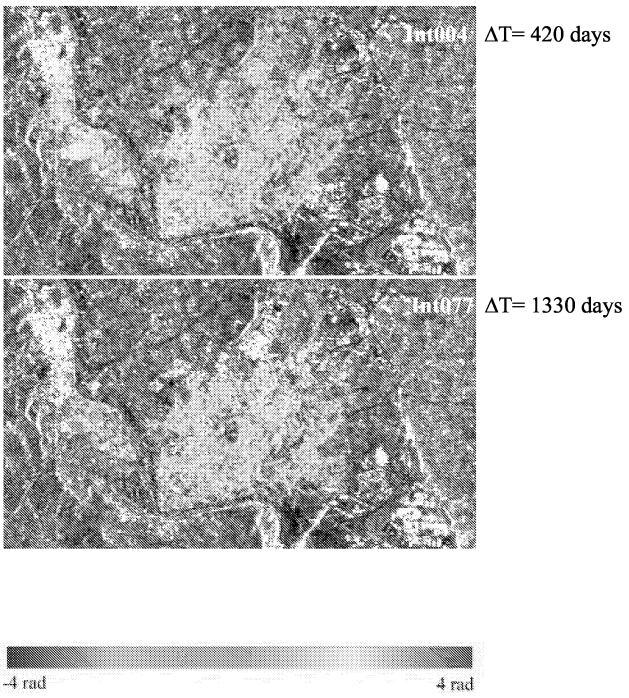

Fig. 2. Autocovariance functions of the DInSAR phase over a stable area (the city of Manresa) of three interferograms (15, 20, 95) with negligible atmospheric components (upper left) and of two interferograms (4, 77) with strong atmospheric components (upper right). Below are illustrated the unwrapped DInSAR phase of the five interferograms.

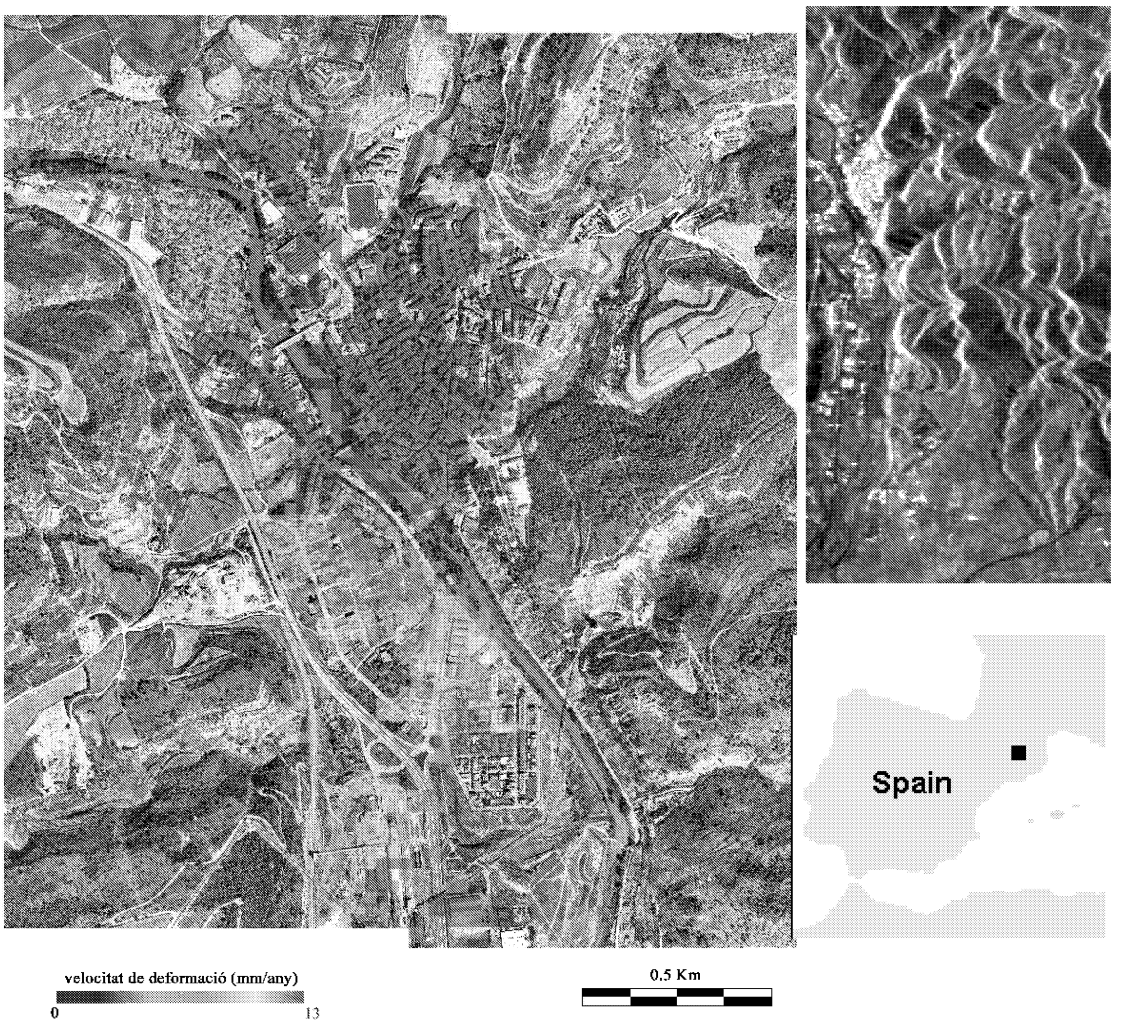

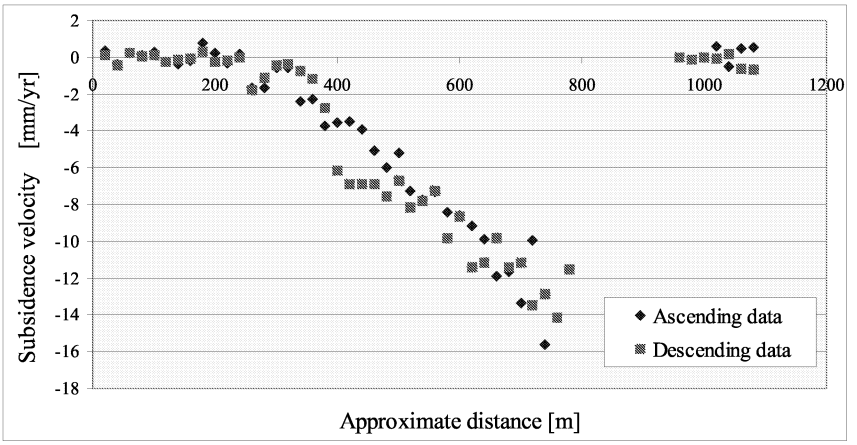

Fig. 3. Sallent test case. Upper left: geocoded mean velocity field estimated with 17 ascending interferometric pairs. The field is superposed to a 1:5000 orthoimage of the Cartographic Institute of Catalonia. Upper right: SAR amplitude (mean amplitude of 14 co-registered images) of an ascending SAR image of the test area. Bottom: comparison of the ascending and descending results, considering the profiles over the two geocoded velocity fields.